Reliable Computation of Local Quantities of Interest in Composite Laminated Plates

P. M. Mohite* and C. S. Upadhyay†
Indian Institute of Technology, Kanpur, Uttar Pradesh 208016, India

In the present study a family of plate models available for the analysis of laminated structures is compared under transverse loading for the point-wise data like maximum transverse deflection and local state of stress. Here, the plate models compared are *Higher-order-Shear-Deformable (HSDT) model, Hierarchic model* and *Layerwise model*. It is seen that all the models predict the deflections accurately. The local state of stress is computed using direct finite element data and equilibrium approach of post processing as well. It is seen for HSDT and hierarchic models that the state of stress computed using direct finite element data is significantly different from exact one, whereas for the layerwise model it is accurately predicted. With equilibrium approach of post processing the local state of stress is accurately predicted by all the models. Further, the effect of the model on first-ply failure load obtained using the equilibrium approach of transverse stress extraction and Tsai-Wu failure criterion is studied. The effect of discretization error control by a one shot adaptive approach has been studied for the first-ply failure loads. It is seen that the control of discretization error together with equilibrium approach of post processing leads to significant reduction in the computed values of failure load.

Nomenclature

x,y,z	=	global coordinates
a,b	=	plate dimensions
t	=	laminate thickness
t_i	=	i^{th} lamina thickness
p_{xy}	=	in-plane approximation order
p_z	=	transverse approximation order
S	=	aspect ratio
q_0	=	intensity of transverse loading
$\mathbf{u}(x,y,z)$	=	generalized displacement
$\bar{z}$	=	non-dimensionalised plate thickness

I. Introduction

THIN structures made of composite laminates are increasingly used in the manufacture of structural components. The enhanced strength to weight ratios make composites especially attractive for aerospace applications. However, being heterogeneous in nature microscopically, the macroscopic behavior of these structures can be complex. One important aspect of the response of laminated structures that a designer should consider is the onset of failure in a laminated structure. Onset of failure in composite laminated plates requires the local stress state to be known in the structure, particularly near structural details; at interlamina interface and in the individual lamina. Accurate prediction of the local stress state becomes important for a reliable estimate of the failure load, which may be crucial for a safe design of the component.

With an increasing demand to maximize payload carrying capabilities of aerial vehicles, shape and topology optimization of structural components has become an important thrust area. All the optimization problems posed in this context are constrained approximation problem with constraints on failure load, maximum transverse deflection, buckling load, natural frequency, etc. In order to obtain an acceptable optimally designed component, from a

* Graduate Student, Department of Aerospace Engineering.
† Assistant Professor, Department of Aerospace Engineering; shekhar@iitk.ac.in.

computational analysis, it becomes imperative to estimate the constraint quantities accurately, at each step of the optimal design process.

The goal of this study is to determine the quality of the local quantities of interest, obtained using various families of plate models commonly used in engineering practice. The comparisons will be done with respect to the exact three-dimensional elasticity solutions, for both symmetric and anti-symmetric stacking of the laminae. The values of the in-plane stresses obtained directly from the finite element computations will be compared to the elasticity solution. For the transverse stress components, the values obtained from the finite element solution directly, and those obtained using the equilibrium approach of post-processing, will be compared to the exact ones. Further, the study aims at clearly demonstrating the need for proper mesh design in the computation of critical failure loads.

II. Plate Models

Several plate theories have been proposed in the literature.[1-3] The goal is generally to give a higher order representation of the transverse shear terms, as in Ref. 1, or to design families of plate theories with guaranteed convergence to the three-dimensional solutions in some norm, as in Ref. 2. However, not much can be said about the accuracy of the local stress state and displacements. In the third type of plate models the individual lamina have continuous through thickness representation of displacements (see Ref. 3). The goal of this study is to determine the quality of the local state of stress, obtained using various families of plate models commonly used in engineering practice. A detailed comparison will be done with respect to the exact three-dimensional elasticity solutions[18-20] for both symmetric and anti-symmetric stacking sequence of the laminae. The values of the in-plane stresses obtained directly from the finite element computations will be compared to the three-dimensional elasticity solution. The effect of model order and in-plane approximation order, on the accuracy of these stresses will be demonstrated. For the transverse stress components, the values obtained from the finite element solution directly, and those obtained using the equilibrium approach of post-processing, will be compared to the exact ones. Further, the study aims at clearly demonstrating the need for proper mesh design in the computation of critical failure loads. Another important goal of this study is to obtain reliable values of the first-ply failure load, using the available models, and compare them with those given in Ref. 22. It will be demonstrated that depending on the applied boundary conditions, stacking sequence and ply orientation, the reliable values of the first-ply failure load can be significantly lower than those obtained using the commonly used meshes and polynomial approximations.

Traditionally, for the plate and shell like thin structures, several plate theories have been proposed. These can be broadly classified as:

1. *higher order shear deformable theories (HSDT);*
2. *hierarchic plate theories* and
3. *layerwise theories*

A. Higher Order Shear Deformable Theories (HSDT)

Here, one such theory due to Reddy[1] is taken as representative theory from this group. It is a third order shear deformable theory with a parabolic distribution of transverse shear strains through thickness of the plate, in order to satisfy the condition of zero transverse shear stress on the top and bottom face of the plate.

B. Hierarchic Plate Theories

In these, the displacement components have a zig-zag or hierarchic representation through the thickness. The hierarchic plate models are a sequence of mathematical models, the exact solutions of which constitute a converging sequence of functions in the norm or norms appropriate for the formulation and objectives of analysis. The construction of hierarchic models for homogeneous isotropic plates and shells was given by Szabó and Sharmann[2] and later for laminated plates by Babuška, Szabó, and Actis[4] and Actis Szabó and Schwab[5]. The solutions of the lower order models are embedded in the highest order model and these models can be adapted according to the requirement.

In these models the displacement field is given as product of functions that depend upon the variables associated with the plate, shell middle surface, and functions of the transverse variable. The transverse functions are derived on the basis of the degree to which the equilibrium equations of three-dimensional elasticity are satisfied. The Fourier transform of the equations of motion is performed which results in two-point boundary value problem for the transverse functions. These are characterized by the geometric parameters and wave vector. These functions are

expanded in powers of wave vector around zero. The transverse functions are obtained by solving equations obtained by substituting the expanded functions into the transformed form of equations of motion.

C. Layerwise Theories

In these theories, the individual lamina has continuous through thickness representation of displacements. In the present study, the layer-by layer model proposed by Ahmed and Basu[3] is adopted. In this model, all the displacement components are represented as product of in-plane and out-of-plane approximating functions of same order. The hierarchic approximating functions were used.

III. Mathematical Formulation of Plate Theories

The generic representation of the displacement field for the plate models is given as:

$$\mathbf{u(x,y,z)} = \begin{Bmatrix} \mathrm{u(x,y,z)} \\ \mathrm{v(x,y,z)} \\ \mathrm{w(x,y,z)} \end{Bmatrix} = [\phi(z)]\mathbf{U}(\mathrm{x,y}) \tag{1}$$

where

$$[\phi(z)] = \begin{bmatrix} \phi_1(z) & 0 & \phi_3(z) & 0 & 0 & \phi_6(z) & 0 & 0 & \cdots \\ 0 & \phi_2(z) & 0 & \phi_4(z) & 0 & 0 & \phi_7(z) & 0 & \cdots \\ 0 & 0 & 0 & 0 & \phi_5(z) & 0 & 0 & \phi_8(z) & \cdots \end{bmatrix} \tag{2}$$

and

$$\{\mathrm{U(x,y)}\} = \{\mathrm{U_1(x,y)U_2(x,y)U_3(x,y)U_4(x,y)\cdots U_8(x,y)}\}^{\mathrm{T}} \tag{3}$$

Note that $U_1(x,y), U_3(x,y), U_6(x,y)\cdots$, ……are the in-plane components of displacement terms $u(x,y,z)$. Similarly, $U_2(x,y), U_4(x,y), U_7(x,y)\cdots$ are the in-plane components of displacement terms $v(x,y,z)$. The in-plane components of transverse displacement $w(x,y,z)$ are given by $U_5(x,y), U_8(x,y)\cdots$. The transverse functions are given in terms of the normalized transverse coordinate $\hat{z} = (2/t)z$ (where t is the thickness of the laminate).

For the higher order shear deformable model the functions $\phi(\hat{z})$ are given as:

$$\phi_1(\mathrm{z}) = \phi_2(\mathrm{z}) = \phi_5(\mathrm{z}) = 1, \;\; \phi_3(\mathrm{z}) = \phi_4(\mathrm{z}) = \mathrm{z},$$

$$\phi_6(\mathrm{z}) = \phi_7(\mathrm{z}) = \phi_8(\mathrm{z}) = \phi_{11}(\mathrm{z}) = 0, \;\; \phi_9(\mathrm{z}) = \phi_{10}(\mathrm{z}) = \mathrm{z}^3$$

Remark: The in-plane displacement components have cubic representation and transverse component is constant in laminate thickness. The quadratic term of in-plane displacement components drop out when the zero shear condition on the top and bottom face of the plate is enforced.

For the hierarchic family of the plate models the transverse functions $\phi(\hat{z})$ are given as:

$$\phi_1(\hat{z}) = \phi_2(\hat{z}) = \phi_5(\hat{z}) = 1; \quad \phi_3(\hat{z}) = \phi_4(\hat{z}) = \hat{z}\frac{t}{2};$$

$$\phi_6(\hat{z}) = \frac{t}{2}\{\varphi_2(\hat{z}) - \varphi_2(0)\}; \quad \phi_7(\hat{z}) = \frac{t}{2}\{\psi_2(\hat{z}) - \psi_2(0)\}; \quad \phi_8(z) = \frac{t}{2}\{\rho_1(\hat{z}) - \rho_1(0)\};$$

$$\phi_9(\hat{z}) = \frac{t^2}{4}\phi_3(\hat{z}); \qquad \phi_{10}(\hat{z}) = \frac{t^2}{4}\psi_3(\hat{z}); \qquad \phi_{11}(\hat{z}) = \frac{t^2}{4}\rho_2(\hat{z})$$

where

$$\varphi_2(\hat{z}) = \int_{-1}^{\hat{z}} \frac{Q_{44} - Q_{45}}{Q_{44}Q_{55} - Q_{45}^2} d\bar{\hat{z}}; \quad \psi_2(\hat{z}) = \int_{-1}^{\hat{z}} \frac{Q_{55} - Q_{45}}{Q_{44}Q_{55} - Q_{45}^2} d\bar{\hat{z}};$$

$$\rho_1(\hat{z}) = \int_{-1}^{\hat{z}} \frac{1}{Q_{13}} d\bar{\hat{z}}$$

Where Q_{ij} are the coefficients of the global constitutive relation, in the global xyz-coordinate system. For other transverse functions see Ref. 5.

The layerwise model used in this paper is adapted from Ref. 3. The present layerwise plate model is an improvement over the model given in Ref. 3, as the original layerwise model had same order transverse representation for all three displacement components, whereas the present layerwise model can have different approximation in transverse direction for individual displacement components. The different approximation for displacement components is used as suggested by Schwab[6], for a single lamina, to take into account the bending and membrane actions. The displacement component u^l, for an element in the l^{th} layer, is given as

$$u^l(x,y,z) = \sum_{j=1}^{(p_{xy}+1)(p_{xy}+2)} \sum_{k}^{p_z^u+1} u_{jk} N_j^l(x,y) M_k^l(z)$$

where p_{xy} and p_z^u are the in-plane and transverse approximation order (for component u^l) and $N_j(x,y)$ and $M_k(z)$ are in-plane and transverse approximation functions, respectively. Similarly the other components v^l and w^l can be expressed. The transverse approximation orders for u and v displacement components will be the same, while that for the component w can be different. Hierarchic basis functions will be used for in-plane and transverse representations of the solution components. In this study, $p_{xy} = 2$ or 3 and p_z^u, $p_z^v = 1$, 2, 3 and $p_z^w = 0$, 1, 2, 3 will be used.

The solution of the plate problem is decomposed into a membrane and a bending part by Schwab.[6] For the membrane part the in-plane displacement components have symmetric representation, whereas, the transverse displacement has anti-symmetric representation. (0,0,1), (2,2,1), (2,2,3) etc. are the transverse representations of displacement components for membrane part in increasing model order. For the bending part, the in-plane displacement components have anti-symmetric representation, whereas, the transverse displacement has symmetric representation. (1,1,0), (1,1,2), (3,3,2) etc. are the transverse representations of displacement components for bending part in increasing model order. When the problem is dominated both by membrane and bending actions then the representations of displacements has to be chosen to satisfy both membrane and bending requirements. In this case (1,1,1), (2,2,2), (3,3,3) etc. representations are used. The authors have developed this capability and implemented it successfully in this study.

Further, In the present study all the displacement components have same order of approximation in the in-plane direction (i.e. the xy-direction).

Remark: The higher-order shear deformation model and hierarchic model do not enforce transverse stress continuity at the interfaces. In the layerwise model the continuity of transverse stress and zero transverse stress on top and bottom faces of laminate can be enforced. Although, in the present layerwise model these conditions are not imposed, it will be shown through numerical examples that the transverse shear stress components show much

smaller (it is close to zero in most of the examples studied) jumps than those computed by using higher-order shear deformable and hierarchic models, and the stresses are close to zero on top and bottom faces of the laminate.

IV. Finite Element Formulation

For a given l^{th} lamina, the constitutive relationship in principal material directions is given as:

$$\{\bar{\sigma}_{(l)}\} = [C_{(l)}]\{\bar{\varepsilon}_{(l)}\} \tag{4}$$

where $\bar{\sigma}_{(l)} = \{\sigma_{11}^{(l)}\ \sigma_{22}^{(l)}\ \sigma_{33}^{(l)}\ \sigma_{23}^{(l)}\ \sigma_{13}^{(l)}\ \sigma_{12}^{(l)}\}^T$ are the stress components for the layer, and $\{\varepsilon_{(l)}\} = \{\varepsilon_{11}^{(l)}\ \ \varepsilon_{22}^{(l)}\ \ \varepsilon_{33}^{(l)}\ \ \gamma_{23}^{(l)}\ \ \gamma_{13}^{(l)}\ \ \gamma_{12}^{(l)}\}^T$ are the components of strain. The subscripts 1, 2 and 3 denote the three principal material directions. The constitutive relationship in global *xyz* coordinates can be obtained by usual transformations.

The potential energy, Π, for the laminate is given by

$$\Pi = \frac{1}{2}\int_V \{\sigma\}\{\varepsilon\}dV \quad -\int_{R^+\cup R^-} q\ w\ ds \tag{5}$$

Where *V* is the volume enclosed by the plate domain, R^+ and R^- are the top and bottom faces of plate and *q(x,y)* is the transverse applied load. The solution to this problem $\mathbf{u}_{ex}$ is the minimizer of the potential energy Π. It is obtained by the solution of following weak problem:

Find $\mathbf{u}_{ex} \in H^\circ(\mathbf{V})$ such that

$$a(\mathbf{u}_{ex}, \mathbf{v}) = f(\mathbf{v}) \quad \forall(\mathbf{v}) \in H^\circ(\mathbf{V}) \tag{6}$$

where $H^\circ(\mathbf{V}) = \{\mathbf{U} = [\phi]U \mid \Phi(\mathbf{u}) < \infty \text{ and } \mathbf{MU} = \mathbf{0} \text{ on } \Gamma_D\}$, Φ is the strain energy with $\Phi = \frac{1}{2}a(\mathbf{u},\mathbf{u})$. Here, $\Gamma = \Gamma_N \cup \Gamma_D$ is the lateral boundary of the plate with Dirichlet part Γ_D and Neumann part Γ_N. Note that in this study Dirichlet means the part of lateral boundary where geometric constraints are imposed, while Neumann stands for the stress-free parts of the lateral boundary. Further, **M** depends on the type of Dirichlet conditions on the edge, i.e. soft-simple support; hard simple-support; clamped etc.

Hence, we have

$$a(\mathbf{u}_{ex}, \mathbf{v}) = \sum_l a_l(\mathbf{u}_{ex}, \mathbf{v}) = \sum_l \int_{V_l} \{\sigma_{(l)}(\mathbf{u}_{ex})\}^T \{\varepsilon_{(l)}(\mathbf{v})\} dV_l$$

and

$$f(\mathbf{v}) = \int_{R^+\cup R^-} q v_3 ds \tag{7}$$

where V_l is the volume of the l^{th} lamina in the laminate; v_3 is the transverse component of test function ***v***.

V. Error Estimator for Local Quantity of Interest

State of stress at a point plays a key role in the first-ply failure analysis of laminates. When the finite element analysis is employed the issue of modeling error (error due to model employed in the analysis of laminate, as compared to three dimensional elasticity) and discretization error becomes important. Adaptive methods for the control of discretization error are available in literature (see Ref. 7-Ref. 9). These are based on the control of energy norm of the error, $\|\mathbf{e}\|_\Omega = \sqrt{2\Phi(\mathbf{e})}$ (where $\Phi(\mathbf{e})$ is the strain energy of the error). This does not guarantee that the

quantity of interest is also accurate. In Ref. 10-Ref. 12 it was shown that the error in the quantity of interest can be given in terms of error in the solution of auxillary problem. The aim of Ref. 12 and Ref. 13 was to control "pollution" error in the quantity of interest. Various smoothening based a-posteriori error estimation techniques for laminated composites have been proposed by the authors for the local quantity of interest.[14] Further, estimation and control of the error in the quantity of interest and "one-shot" adaptive approach for the control of discretization error was proposed in Ref. 15 and used for the accurate analysis of first-ply failure loads in Ref. 16. In the present paper the issue of control of modeling error is not addressed. Reference 17 can be referred as an example for the modeling error. In the following sections the main steps of error estimation for local quantity of interest and one shot adaptivity are given from Ref. 15.

A. Definition of Error Estimator

The variational formulation in Eq. (7) is used to obtain the finite element solution $\mathbf{u}_h \in \mathbf{H}_h^{\circ}(\mathbf{V})$, where $\mathbf{H}_h^{\circ}(\mathbf{V}) = \left\{ \mathbf{u} = [\phi]\mathbf{U};\ U_i \in S_\tau^{p_{xy}},\ i = 1,2,3\cdots \mid \blacklozenge(\mathbf{u}) < \infty,\ \mathbf{MU} = \mathbf{0} \text{ on } \Gamma_D \right\}$.

Letting ϖ_{2D} be the plate mid surface with boundary $\partial\varpi_{2D}$, we define $S_\tau^{p_{xy}}$ as the set of globally continuous piecewise polynomials of order p_{xy} over each element $\tau\ (\tau \in \varpi_{2D})$.

$$\blacktriangleleft(\mathbf{u}_h, \mathbf{v}_h) = \blacktriangleright(\mathbf{v}_h) \quad \forall\ \mathbf{v}_h \in \mathbf{H}_h^{\circ}(\mathbf{V}) \tag{8}$$

Note that $\mathbf{u}_h = [\phi]\mathbf{U}_h$ is the representation of $\mathbf{u}_h$, following (1). The error in the solution can be given as $\mathbf{e} = \mathbf{u}_{ex} - \mathbf{u}_h$. An approximation to the error can be given as $\mathbf{e}^* = \mathbf{u}^* - \mathbf{u}_h$ where $\mathbf{u}^* \in S_\tau^{p_{xy}+k}$ is obtained for each element τ as described below (see Ref. 14 for details). In all the numerical examples $k = 2$ has been employed.

For an element τ let P_τ be the patch of elements in a one-layer neighborhood of τ, as shown in Fig. 1.

Over the patch P_τ, define

$\mathbf{u}^* = \begin{Bmatrix} u^* \\ v^* \\ w^* \end{Bmatrix} = [\phi]\mathbf{U}^*$ where $U_i^* = \sum_{j=1}^{NDOF} A_{ij} q_j(x,y)$ with $NDOF = (p_{xy}+1+k)(p_{xy}+2+k)/2$; $q_j(x,y)$ as the monomials of order $\le p_{xy} + k$ (see Ref. 14 for details) defined in terms of local coordinates $\hat{x} = x - x_c^\tau$, $\hat{y} = y - y_c^\tau$. Here x_c^τ, y_c^τ are the centroidal coordinates for element τ. The $q_j(x,y)$ can be given as:

$$\begin{aligned} &q_1(x,y) = 1, \quad q_2(x,y) = \hat{x}, \quad q_3(x,y) = \hat{y}, \\ &q_4(x,y) = \hat{x}^2, \quad q_5(x,y) = \hat{x}\hat{y}, \quad q_6(x,y) = \hat{y}^2 \quad \cdots \end{aligned} \tag{9}$$

The coefficients A_{ij} are obtained by minimizing $J = \frac{1}{2}\int_{A_{P_\tau}} |\mathbf{U}^* - \mathbf{U}_h|^2\, dA$ where A_{P_τ} is the area of the patch P_τ (where $A_{P_\tau} \subset \varpi_{2D}$). This definition is called the L_2 projection based error estimator (see Ref. 14 for details).

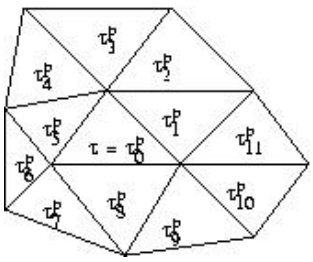

Fig. 1 One layer neighborhood patch around element τ

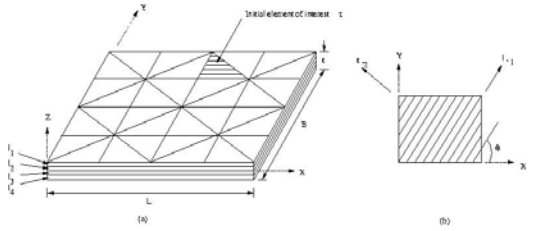

Fig. 2 Plate domain

B. Auxillary Problem

Let us consider the domain of Fig. 2. Let us further assume that we are interested in the value of stress component σ_{yy} in the topmost layer, for all points in the element τ (shown in Fig. 2).

In order to accurately obtain the pointwise information in τ, we will let $\sigma^{(l)}_{yy,avg} = \frac{1}{V^l_\tau}\int_{V^l_t} \sigma_{yy} dv$ as the quantity of interest. Here, $V^l_\tau = A_\tau t_l$ is the volume enclosed by the element τ in the l^{th} layer. Hence,

$$\sigma^{(l)}_{yy,avg} = \frac{1}{A_\tau t_l}\int_{z=z_{l-1}}^{z_l}\int_{A_\tau}(\sigma_{yy} dA)dz \tag{10}$$

with t_l as the thickness of the l^{th} layer; z_{l-1} and z_l as the lower and upper z coordinates for the l^{th} layer; A_τ is the area of element τ (or group of elements).

Remark: In this study, the quantity of interest used is the stress component which contributes maximum to the failure index for the Tsai-Wu criterion.

Corresponding to $\sigma^{(l)}_{yy,avg}$ we define the following auxillary problem:

Find $\mathbf{G} \in \mathbf{H}^{\circ}(\mathbf{V})$ such that

$$\aleph(\mathbf{G}, \mathbf{v}) = \sigma^{(l)}_{yy,avg}(\mathbf{v}) = \beth(\mathbf{v}) \;\forall\; \mathbf{v} \in \mathbf{H}^{\circ}(\mathbf{V}) \tag{11}$$

Letting $\mathbf{G}_h \in \mathbf{H}^{\circ}_h(\mathbf{v})$ be the finite element solution for $\mathbf{G}$, we have

$$\aleph(\mathbf{G}_h, \mathbf{v}_h) = \sigma^{(l)}_{yy,avg}(\mathbf{v}_h) = \beth(\mathbf{v}_h) \;\forall\; \mathbf{v} \in \mathbf{H}^{\circ}_h(\mathbf{V}) \tag{12}$$

Note that $\mathbf{u}_h$ and $\mathbf{G}_h$ can be solved simultaneously (see Ref. 15). Multiple regions can be handled simultaneously.

C. Estimators for Error in Quantity of Interest

From the previous section we have:

$$\aleph(\mathbf{G}, \mathbf{u}_{ex} - \mathbf{u}_h) = \beth(\mathbf{u}_{ex}) - \beth(\mathbf{u}_h) = \beth(\mathbf{u}_{ex} - \mathbf{u}_h) = \beth(\mathbf{e}) \tag{13}$$

From the orthogonality property of the error in the finite element solution, we have:

$$|\aleph(\mathbf{G} - \mathbf{G}_h, \mathbf{u}_{ex} - \mathbf{u}_h)| = |\beth(\mathbf{e})| \tag{14}$$

or

$$|\beth(\mathbf{e})| = |\aleph(\mathbf{G} - \mathbf{G}_h, \mathbf{u}_{ex} - \mathbf{u}_h)| \le \sum_\tau |\aleph(\mathbf{G} - \mathbf{G}_h, \mathbf{u}_{ex} - \mathbf{u}_h)| \le \sum_\tau \|\mathbf{e_u}\|_\tau \|\mathbf{e_G}\|_\tau \le \|\mathbf{e_u}\| \|\mathbf{e_G}\| \tag{15}$$

where $\mathbf{e_u} = \mathbf{e}$ stands for the error in the actual solution and $\mathbf{e_G}$ stands for the error in the auxillary problem.

D. Definition of a-posteriori Error Estimators for Local Quantity of Interest

Replacing $\mathbf{e_u}$ with $\mathbf{e^*_u}$ and $\mathbf{e_G}$ with the estimate $\mathbf{e^*_G}$, we can get many definitions of the estimators (see Ref. 15), for the error in the quantity of interest. Here we employ

Estimator (*E*):

$$|\mathcal{F}(\mathbf{e})|_E = \sum_{\tau} |\mathcal{B}(\mathbf{e}_{\mathbf{u}}^*, \mathbf{e}_{\mathbf{G}}^*)| \tag{16}$$

E. One Shot Adaptivity for Quantity of Interest

We let $\mathbf{u}_h^{(p_{xy})}$, $\mathbf{G}_h^{(p_{xy})}$ be the finite element solutions of the order p_{xy} for $\mathbf{u}_{ex}$ and $\mathbf{G}$. Thus, we can approximate error $\mathbf{e}_{\mathbf{u}}$ as $\mathbf{e}_{\mathbf{u}} \approx \mathbf{e}_{\mathbf{u}}^{(p_{xy}+1)} = \mathbf{u}_h^{(p_{xy}+1)} - \mathbf{u}_h^{(p_{xy})}$ and hence $\mathcal{F}(\mathbf{e}) \approx \mathcal{F}\left(\mathbf{e}_{\mathbf{u}}^{(p_{xy}+1)}\right)$. It can be shown that $\mathcal{F}\left(\mathbf{e}_{\mathbf{u}}^{(p_{xy}+1)}\right) = \sum_{\tau} \mathcal{B}\left(\mathbf{e}_{\mathbf{G}}^{(p_{xy}+1)}, \mathbf{e}_{\mathbf{u}}^{(p_{xy}+1)}\right)$.

Letting τ be the element of interest and *P* the one-layer neighborhood of τ, the total error can be partitioned into two parts as follows:

$$|\mathcal{F}(\mathbf{e})| \leq |\mathcal{F}_1(\mathbf{e})| + |\mathcal{F}_2(\mathbf{e})|$$

where

$$\mathcal{F}_1(\mathbf{e}) = \sum_{\tau \in P} \mathcal{B}(\mathbf{e}_{\mathbf{u}}, \mathbf{e}_{\mathbf{G}}), \quad \mathcal{F}_2(\mathbf{e}) \sum_{\tau \in P'} \mathcal{B}(\mathbf{e}_{\mathbf{u}}, \mathbf{e}_{\mathbf{G}}) \tag{17}$$

where P' is the set of elements lying outside *P*. Following Ref. 12, $\mathcal{F}_1(\mathbf{e})$ is the local part of the error and $\mathcal{F}_2(\mathbf{e})$ is the "pollution" in the quantity of interest (i.e. far-field influence). Following Ref. 13 and Ref. 15, we have:

$$|\mathcal{F}_1(\mathbf{e})| \leq \sum_{\tau \in P} \|\mathbf{e}_{\mathbf{u}}\| \|\mathbf{e}_{\mathbf{G}}\| \leq C h^{p_{xy}} \tag{18}$$

Beyond P, the auxillary function is well behaved and hence

$$|\mathcal{F}_2(\mathbf{e})| \leq \sum_{\tau \in P'} \|\mathbf{e}_{\mathbf{u}}\| \|\mathbf{e}_{\mathbf{G}}\| \leq C h^{2p_{xy}} \tag{19}$$

The goal of the adaptive process is to refine the given mesh selectively such that the total error is below the specified tolerance, i.e.

$$|\mathcal{F}(\mathbf{e})| \leq \eta |\mathcal{F}(\mathbf{u}_h)| \tag{20}$$

where $|\mathcal{F}(\mathbf{u}_h)|$ is the computed value of the desired quantity of interest; $|F(e)| = |F(e)|_E$ is obtained using definition *E* for the error. Following Ref. 8, we will define $r_\tau = \frac{h_d}{h}$ as the ratio of the desired (h_d) to the actual mesh size (*h*) of the element τ. The desired mesh should have the least number of elements, of all possible meshes. Hence, following Ref. 8, Ref. 15, we minimize

$$\sum_{\tau} \frac{1}{r_\tau^2} \tag{21}$$

subject to constraint Eq. (20). Thus, we define new objective function (to be minimized) as,

$$J = \sum_{\tau} \frac{1}{r_{\tau}^2} + \lambda_1 \left(\sum_{\tau \in P} \chi_{d,\tau}^2 - \eta_{d,1} \right) + \lambda_2 \left(\sum_{\tau \in P'} \chi_{d,\tau}^2 - \eta_{d,2} \right) \tag{22}$$

where $\chi_{d,\tau} = |\mathcal{E}(\hat{\mathbf{e}}_{\mathbf{u}}, \hat{\mathbf{e}}_{\mathbf{G}})|$ is the desired contribution to the total error from element τ; $\hat{\mathbf{e}}_{\mathbf{u}}$, $\hat{\mathbf{e}}_{\mathbf{G}}$ are the desired errors in the element τ; λ_1 and λ_2 are the Lagrange multipliers; $\eta_{d,1} = \eta_1 |\eta(\mathbf{u}_h)|$ and $\eta_{d,2} = \eta_2 |\eta(\mathbf{u}_h)|$ are the desired errors in the region *P* and P', respectively (here $\eta = \eta_1 + \eta_2$). Using Eq. (18) and Eq. (19) $\chi_{d,\tau}^2$ can be given in terms of the actual error $\chi_{a,\tau}^2$ (where $\chi_{a,\tau}^2 = |\mathcal{E}(\mathbf{e}_{\mathbf{u}}, \mathbf{e}_{\mathbf{G}})|$ in the element τ), as

$$\text{For } \tau \in P \quad \chi_{d,\tau}^2 = r_{\tau}^{p_{xy}} \chi_{a,\tau}^2$$

$$\text{For } \tau \in P' \quad \chi_{d,\tau}^2 = r_{\tau}^{2p_{xy}} \chi_{a,\tau}^2$$

Thus (22) becomes

$$J = \sum_{\tau} \frac{1}{r_{\tau}^2} + \lambda_1 \left(\sum_{\tau \in P} r_{\tau}^{p_{xy}} \chi_{a,\tau}^2 - \eta_{d,1} \right) + \lambda_2 \left(\sum_{\tau \in P'} r_{\tau}^{2p_{xy}} \chi_{a,\tau}^2 - \eta_{d,2} \right) \tag{24}$$

Minimizing *J* with respect to r_{τ}, λ_1 and λ_2 we get:

For $\tau \in P$,

$$r_{\tau} = \frac{\eta_{d,1}^{1/p_{xy}}}{\left(\sum_{\tau \in P} \chi_{a,\tau}^{4/(p_{xy}+2)} \right)^{1/p_{xy}} \chi_{a,\tau}^{2/(p_{xy}+2)}} \tag{25}$$

For $\tau \in P'$

$$r_{\tau} = \frac{\eta_{d,2}^{1/2p_{xy}}}{\left(\sum_{\tau \in P'} \chi_{a,\tau}^{2/(p_{xy}+1)} \right)^{1/2p_{xy}} \chi_{a,\tau}^{1/(p_{xy}+1)}} \tag{26}$$

Using the computed values of r_{τ}, the desired mesh sizes can be computed. The mesh can be locally refined several times based on the desired mesh size. This leads to a final adaptively refined mesh.

Remark: The partition of the contribution to the error from *P* and P' is based on the user. The final mesh depends on the choice of η_1 and η_2. In this study $\eta_1 = \eta_2 = \eta/2$ is taken. In all the computations in this study, $\eta = 10\%$ is used.

VI. Tsai-Wu Failure Criterion

It is a complete polynomial criterion and is an extension of the criterion used for anisotropic materials (see Ref. 18).

The Tsai-Wu criterion is given by

$$FI_{TW} = F_i \sigma_i + F_{ij} \sigma_i \sigma_j \geq 1 \tag{27}$$

where $F_{i,}$ F_{ij} are the strength tensor terms and σ_i are the stress components and

$$F_1 = \frac{1}{X_T} - \frac{1}{X_C};\ F_2 = \frac{1}{Y_T} - \frac{1}{Y_C};\ F_3 = \frac{1}{Z_T} - \frac{1}{Z_C}$$

$$F_{11} = \frac{1}{X_T X_C};\ F_{22} = \frac{1}{Y_T Y_C};\ F_{33} = \frac{1}{Z_T Z_C}$$

$$F_{44} = \frac{1}{R^2};\ F_{55} = \frac{1}{S^2};\ F_{66} = \frac{1}{T^2}$$

$$F_{12} = -\frac{1}{2}\sqrt{X_T X_C Y_T Y_C};\ F_{13} = -\frac{1}{2}\sqrt{X_T X_C Z_T Z_C};\ F_{23} = -\frac{1}{2}\sqrt{Y_T Y_C Z_T Z_C} \tag{28}$$

where X, Y and Z are strengths in 1, 2 and 3 directions, respectively. Subscript T denotes tensile strength, and C denotes compressive strength. R, S and T are shear strengths in 12, 13, and 23 planes, respectively.

VII. Numerical Results

One of the main goals of this study is to compare the various families of plate models, with respect to the quality of the pointwise stresses obtained using the models. All the models are compared for the transverse maximum deflection and stress profiles for various ply orientations, stacking sequences and boundary conditions under transverse loadings. In the present study, three types of transverse loadings are considered: uniform pressure, sinusoidal and cylindrical bending.

In the first section of numerical results, the effect of plate models on the accuracy of pointwise data i.e. transverse deflection and all the stress components at a point, is addressed. The stress components are either directly computed using constitutive equations, or the equilibrium approach to obtain transverse normal and shear stresses.

In the second section, the effect of the plate models on the accuracy of first-ply failure load is addressed.

Effect of Models on Accuracy of Pointwise Data

Comparison of Transverse Deflection

In this section the transverse deflection component obtained using different plate models and in-plane discretization is compared with the exact three-dimensional elasticity results reported in Ref. 19, for cross-ply laminate sequence with material properties given in Table 1. The plate has dimension a along x-axis and b along y-axis, and is subjected to sinusoidal loading of the form

$$q(x,y) = q_0(x,y)\sin\left(\frac{\pi x}{a}\right)\sin\left(\frac{\pi y}{b}\right) \tag{29}$$

All edges of the plate are simply supported (see Table 2 for all BC's used). The transverse deflection at $\left(\frac{a}{2},\frac{b}{2},0\right)$ is reported in Tables 3 and 4. Note that in all the computations the layerwise model uses (3,3,2) model (unless specified), that is, transverse approximation for u and v is cubic and quadratic for w. For the hierarchic family 11 field model is used, while for the HSDT model (3,3,0) approximation is used. Square plate with cross ply laminae, such that outer laminae have orientation 0°, and total thickness of 0° laminae is equal to total thickness of 90° laminae. Also laminae with same orientation have equal thickness. In this study, 7 and 9-layered laminate is studied. The transverse deflection is nondimensionalised as $w^* = \frac{\pi^4 Q w}{12 q_0 S^4 t}$, where $Q = 4G_{12} + \left[E_{11} + E_{22}\left(1 + 2\nu_{23}\right)\right]/\left(1 - \nu_{12}\nu_{21}\right)$. Here, $p_{xy} = 3$ is used for all models. Numbers in parenthesis show the % error with respect to exact solution.

From tables 3 and 4 we observe that:

1. The layerwise model predicts the transverse deflection accurately for all the aspect ratios. The error in the values ranges from 0-0.15 %.

2. The HSDT and hierarchic model are far from the exact one for the aspect ratios upto $S = 10$. The error for this aspect ratios ranges from 5-16 %.
3. For the HSDT and hierarchic model with aspect ratios $S > 10$ the displacement is close to exact. The error is 0.1-3 %.
4. The hierarchic theory is closer to the exact one; as compared to the higher order shear deformable theories.

Table 1 Material Properties for Ref. 18-Ref. 20.

Property	E_1	E_2	G_{12}	G_{23}	$\upsilon_{12}=\upsilon_{23}$
Value	25×10^6 psi	10^6 psi	0.5×10^6 psi	0.2×10^6 psi	0.25

Table 2: Boundary conditions

Boundary Condition	At y=0 and y=b	At x=0 and x=a
Soft Simple Support	v=w=0	u=w=0
Clamped	u=v=w=0	u=v=w=0
Free	u, v, w≠0	u, v, w≠0

Table 3:Non-dimensional transverse deflection $\left(w^*\right)$ for 7 layered cross-ply laminate.

S	Pagano[19]	Layer-wise	HSDT	Hierarchic
2	12.342	12.341 (0.00)	10.918 (11.54)	10.358 (16.07)
4	4.153	4.153 (0.00)	3.594 (13.46)	3.575 (13.92)
10	1.529	1.529 (0.00)	1.417 (7.33)	1.444 (5.56)
20	1.133	1.133 (0.00)	1.096 (3.26)	1.113 (1.76)
50	1.021	1.021 (0.00)	1.005 (1.56)	1.017 (0.39)
100	1.005	1.005 (0.00)	0.993 (1.19)	1.004 (0.09)

Table 4:Non-dimensional transverse deflection $\left(w^*\right)$ for 9 layered cross-ply laminate.

S	Pagano[19]	Layer-wise	HSDT	Hierarchic
2	12.288	12.306 (-0.15)	10.703 (12.89)	11.632 (5.34)
4	4.079	4.079 (0.00)	3.530 (13.46)	3.664 (10.17)
10	1.512	1.512 (0.00)	1.406 (7.01)	1.438 (4.89)
20	1.129	1.129 (0.00)	1.093 (3.18)	1.110 (1.68)
50	1.021	1.020 (0.09)	1.001 (1.96)	1.017 (0.39)
100	1.005	1.005 (0.00)	1.004 (0.09)	0.993 (1.19)

Comparison of Stresses

Here, various stress components for symmetric and antisymmetric laminates, under cylindrical bending, are compared with the exact values given in Ref. 19-Ref. 21.

Case 1: In this case [0/90/0], square laminate with all edges simple supported is considered. All the laminae are of equal thickness. The sinusoidal loading is of the same form as above. The in-plane stresses are nondimensionalised as $\left(\bar{\sigma}_{xx},\bar{\sigma}_{yy},\bar{\tau}_{xy}\right)=\frac{1}{q_0 S^2}\left(\sigma_{xx}\left(\frac{a}{2},\frac{b}{2},\bar{z}\right),\sigma_{yy}\left(\frac{a}{2},\frac{b}{2},\bar{z}\right),\tau_{xy}\left(0,0,\bar{z}\right)\right)$ and the transverse stresses as $\left(\bar{\tau}_{xz},\bar{\tau}_{yz}\right)=\frac{1}{q_0 S}\left(\tau_{xz}\left(0,\frac{b}{2},\bar{z}\right),\tau_{yz}\left(\frac{a}{2},0,\bar{z}\right)\right)$. The in-plane stress components are shown in Fig. 3 and transverse stress component is shown in Fig. 4.

Case 2: In this case, [165/-165] laminate under cylindrical loading is considered. The loading is of the form $q(x,y) = q_0(x)\sin\left(\frac{\pi x}{a}\right)$. The plate is infinite along y-direction. All the laminae are of equal thickness. The stress components are nondimensionalised as $(\bar{\sigma}_{xx}) = \frac{1}{q_0 S^2}\left(\sigma_{xx}\left(\frac{a}{2}, \bar{z}\right)\right)$ and $(\bar{\tau}_{xz}, \bar{\tau}_{yz}) = \frac{1}{q_0 S}(\tau_{xz}(0,\bar{z}), \tau_{yz}(0,\bar{z}))$. The in-plane stress components are shown in Fig. 5 and transverse stress components are shown in Fig. 6.

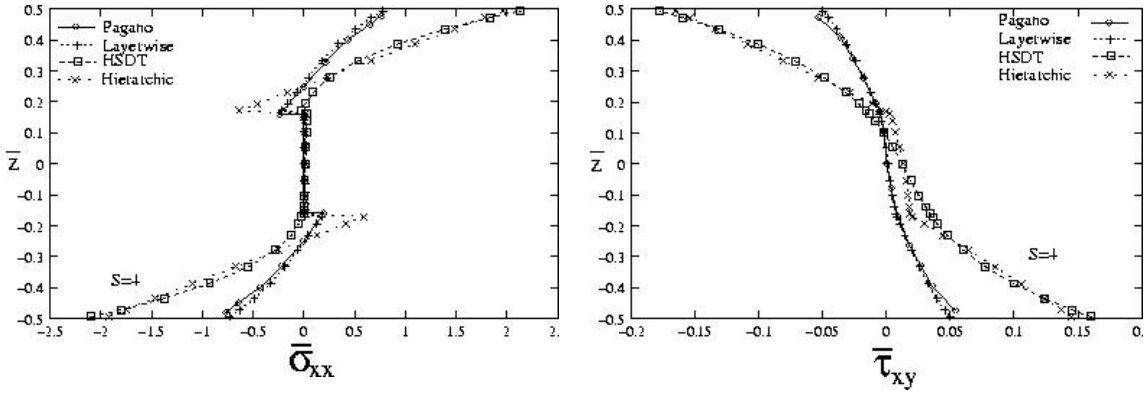

Fig. 3 [0/90/0] laminate; all edges simply supported, in-plane stresses.

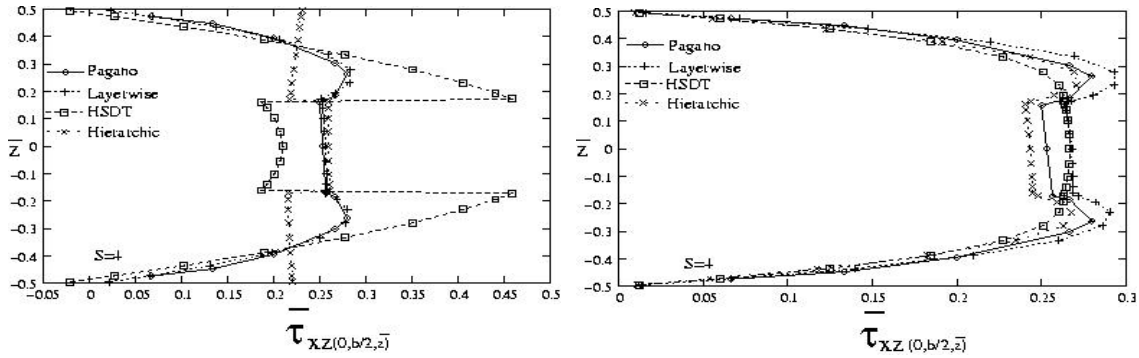

Direct stresses Equilibrium stresses

Fig. 4 [0/90/0] laminate; all edges simply supported, transverse stresses.

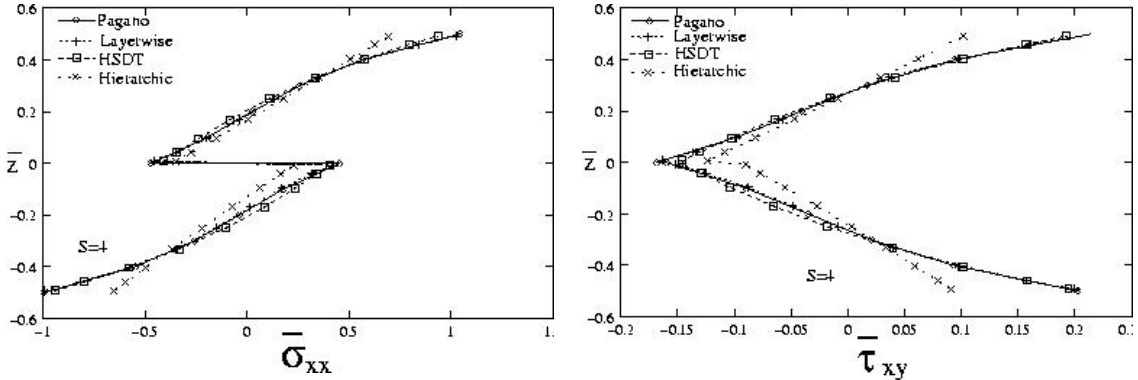

Fig. 5 [165/-165] laminate under cylindrical bending, in-plane stresses.

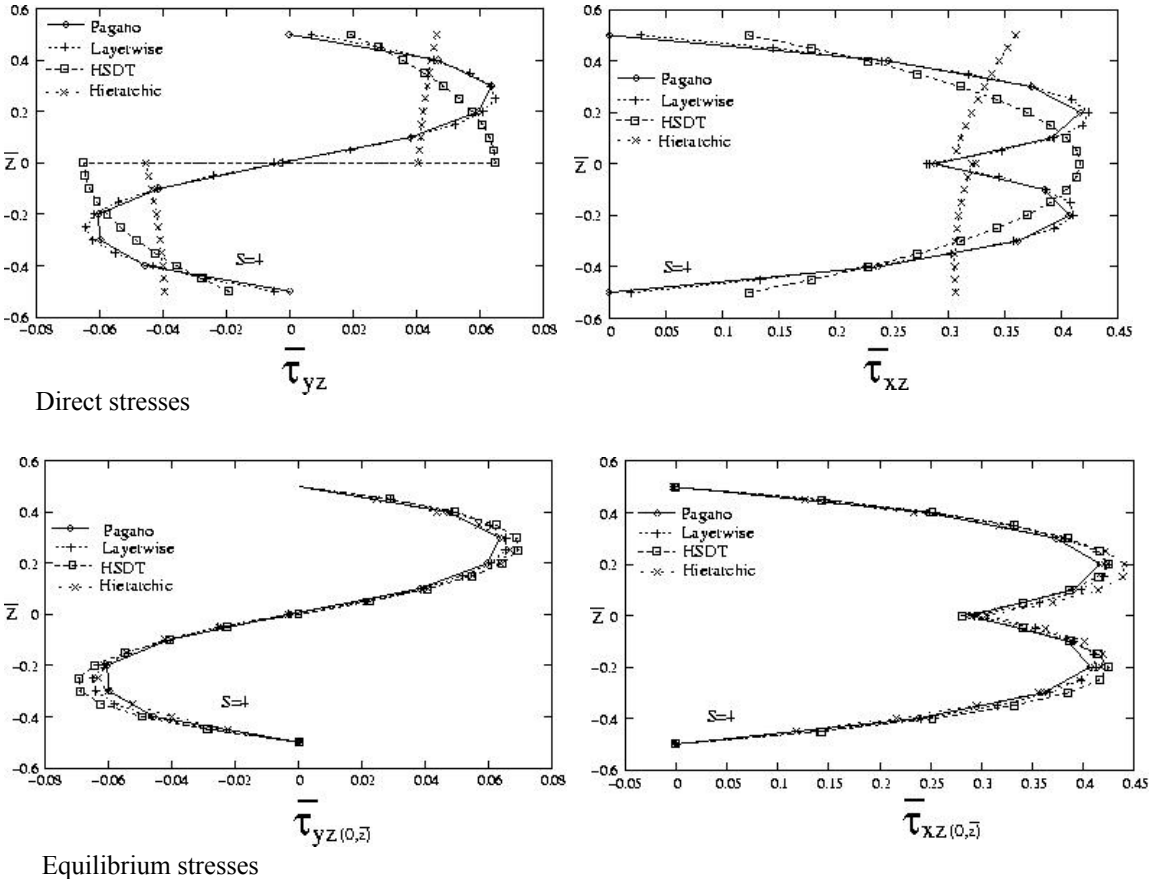

Fig. 6 [165/-165] laminate under cylindrical bending, transverse stresses.

Case 3: The problem description is same as previous sub-subsection. The stress components are nondimensionalised as case 1 above. The point-wise stress values are given for layerwise model in Tables 5 and 6. In these tables the first row gives the value at $\bar{z} = 0$ while in the second maximum values and in the third row their location quoted in parenthesis is reported for the components τ_{xz} and τ_{yz}.

From the results it is observed that:

1. The in-plane stress components are accurately predicted by all higher order models.
2. The transverse shear stress components computed directly from finite element solution is accurate for the layerwise model whereas, those obtained by HSDT and hierarchic models are significantly different both qualitatively and quantitatively.
3. Using the equilibrium approach of post-processing leads to more accurate transverse stress components for all the models.
4. The layerwise model predicts accurately the point-wise values of the stress components for all the values of S.

Effect of Models on Accuracy of Predicted Failure Load

The laminates considered are $[0/90]_S$ and [-45/45/-45/45]. The plate is either clamped on all edges or simple supported. The top face of the plate is subjected to uniform transverse load $q(x,y) = q_0$. The plate dimensions are $a = 228.9\ mm\ (9\,in)$ and $b = 127\ mm\ (5\ in)$. The material properties are given in Table 7. The first-ply failure load is nondimensionalised as $FLD = \dfrac{q_0}{E_{22}} S^4$. The results obtained from the present analysis are compared with those reported in Ref. 22.

Table 5:Comparison of non-dimensional stresses for 7 layered cross-ply laminate.

S	$\sigma_{xx}(\frac{a}{2},\frac{a}{2},\pm\frac{1}{2})$		$\sigma_{yy}(\frac{a}{2},\frac{a}{2},\pm\frac{3}{8})$		$\tau_{xz}(0,\frac{a}{2},0)$		$\tau_{yz}(\frac{a}{2},0,0)$		$\tau_{xy}(0,0,\pm\frac{1}{2})$	
	Exact	Layer	Exact	Layer	Exact	Layer	Exact	Layer	Exact	Layer
	1.284	1.287	1.039	1.040	0.178	0.177	0.238	0.238	-0.0775	-0.0776
2	-0.880	-0.882	-0.838	-0.839	0.229	0.229	0.239	0.240	0.0579	0.0580
					(0.16)	(0.16)	(0.02)	(0.02)		
	0.679	0.678	0.623	0.623	0.219	0.219	0.236	0.237	-0.0356	-0.0357
4	-0.645	-0.646	-0.610	-0.610	0.223	0.223			0.0347	0.0347
					(0.12)	(0.12)				
	0.548	0.548	0.457	0.457	0.255	0.255	0.219	0.220	-0.0237	-0.0237
10	-0.548	-0.549	-0.458	-0.458	0.255	0.255			0.0238	0.0239
					(-0.02)	(-0.02)				
20	0.539	0.540	0.419	0.420	0.267	0.267	0.210	0.214	-0.0219	-0.0219
	-0.539	-0.541	-0.420	-0.420					0.0219	0.0220
50	0.539	0.541	0.407	0.408	0.271	0.277	0.206	0.0225	-0.0214	-0.0215
	-0.539	-0.541	-0.407	-0.408					0.0214	0.0215
100	0.539	0.545	0.405	0.409	0.272	0.291	0.205	0.262	-0.0213	-0.0216
	-0.539	-0.545	-0.405	-0.409					0.0213	0.0216

Table 6:Comparison of non-dimensional stresses for 9 layered cross-ply laminate.

S	$\sigma_{xx}(\frac{a}{2},\frac{a}{2},\pm\frac{1}{2})$		$\sigma_{yy}(\frac{a}{2},\frac{a}{2},\pm\frac{3}{8})$		$\tau_{xz}(0,\frac{a}{2},0)$		$\tau_{yz}(\frac{a}{2},0,0)$		$\tau_{xy}(0,0,\pm\frac{1}{2})$	
	Exact	Layer	Exact	Layer	Exact	Layer	Exact	Layer	Exact	Layer
	1.260	1.263	1.051	1.052	0.204	0.204	0.194	0.194	-0.0722	-0.0723
2	-0.866	-0.868	-0.824	-0.825	0.224	0.224	0.211	0.229	0.0534	0.0535
					(0.23)	(0.235)	(-0.1)	(0.1)		
	0.684	0.685	0.628	0.628	0.223	0.223	0.223	0.223	-0.0337	-0.0338
4	-0.649	-0.650	-0.612	-0.612	0.223	0.223	0.225	0.226	0.0328	0.0329
					(0.01)	(0.01)	(-0.06)	(±0.08)		
	0.551	0.552	0.477	0.477	0.247	0.247	0.226	0.226	-0.0233	-0.0234
10	-0.551	-0.552	-0.477	-0.477			0.226	0.227	0.0235	0.0235
							(-0.01)	(±0.05)		
	0.541	0.542	0.444	0.444	0.255	0.255	0.221	0.223	-0.0218	-0.0219
20	-0.541	-0.542	-0.444	-0.444				0.224	0.0218	0.0219
								(±0.05)		
	0.539	0.542	0.433	0.435	0.258	0.262	0.219	0.232	-0.0214	-0.0215
50	-0.539	-0.542	-0.433	-0.433				0.237	0.0214	0.0215
								(±0.05)		
	0.539	0.546	0.431	0.436	0.256	0.266	0.219	0.258	-0.0213	-0.0216
100	-0.539	-0.546	-0.431	-0.436		0.273		0.275	0.0213	0.0216
						(±0.05)		(0.05)		

Table 7: Material properties for T300/5208 Graphite/Epoxy (Pre-preg) (Ref.21).

Property	Value	Property	Value
E_{11}	132.5 GPa	X_T	1515 MPa
$E_{22} = E_{33}$	10.8 GPa	X_C	1697 MPa
$G_{12} = G_{13}$	5.7 GPa	$Y_T = Y_C = Z_T = Z_C$	43.8 MPa
G_{23}	3.4 GPa	R	67.6 MPa
$\nu_{12} = \nu_{13}$	0.24	$S = T$	86.9 MPa
ν_{23}	0.49	Ply thickness, t_i	0.127 mm

The computed failure load depends on the accuracy of the lamina level stress. In general, there is no a-priori information about the quality of the local stress. Hence, an adaptive approach with the capability to estimate error in the local stresses and refine mesh accordingly to bring the error down to acceptable tolerance, is devised. For the fixed model, the focussed adaptive approach (as discussed in earlier section) is employed to recompute the failure load. Here, the stress component contributing maximum to the Tsai-Wu first-ply failure criterion is used as the quantity of interest. In Tables 8-15 the first-ply failure loads are given. In these tables,

1. The superscript a shows all the values of failure loads and corresponding failure index obtained using mesh shown in Fig.7a.
2. The superscript b shows the value of the failure index obtained with the same load as in a and the adapted mesh. (e.g. see Fig.7b).
3. The superscript c shows the first-ply failure load for the adapted mesh. The initial mesh and final adapted mesh for HSDT and hierarchic models for a representative problem are shown in Fig. 7b,c,d.

Note that the first-ply failure load for layerwise model is computed using only the initial mesh. In the present study, the stress components obtained directly from the finite element computation, as well as the transverse components obtained from the equilibrium approach, have been used in computing the failure load.

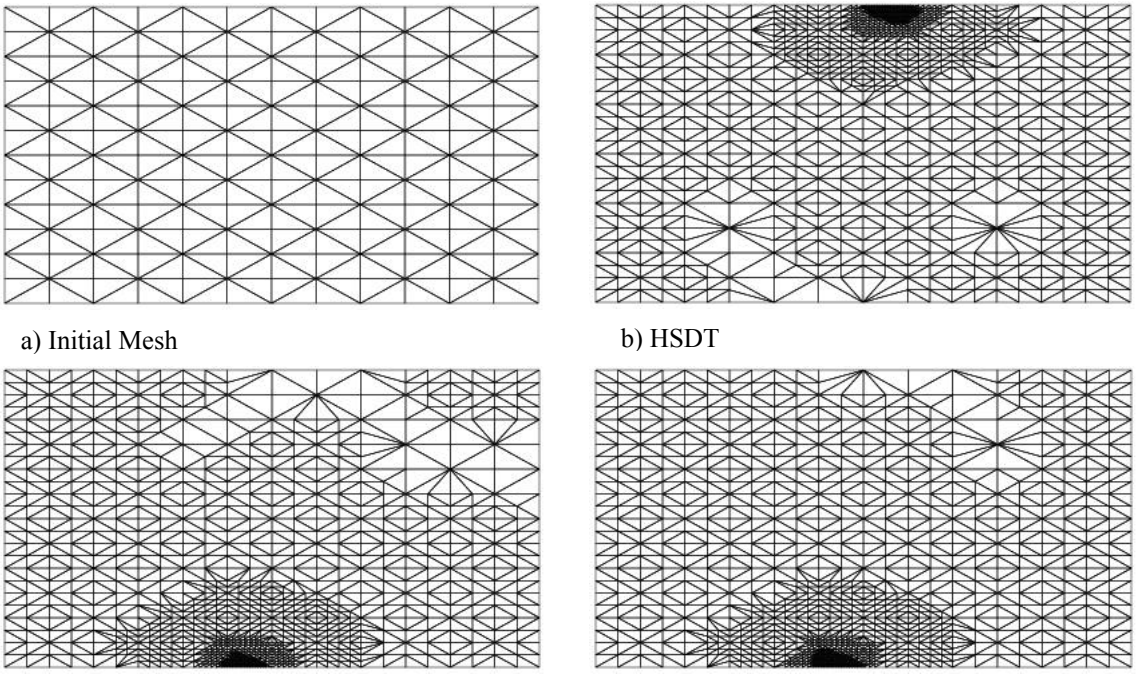

a) Initial Mesh

b) HSDT

c) 8-field

d) 11-field

Fig. 7 Adapted meshes for $[0/90]_S$ clamped laminate.

Table 8: First-ply failure loads; all edges clamped, $[0/90]_S$ laminate under uniform transverse loading, (direct stresses) $p_{xy} = 2$.

Model	FLD	Xco	Yco	Layer	Location	FI_{TW}	Max. σ
Reddy[22]	19050.9	≈5.00	≈65.00	1	bottom	-	
HSDT[a]	20265.4	112.04	0.67	1	bottom	1.00	σ_{yy}
HSDT[b]	20265.4	113.85	0.16	1	bottom	1.82	
HSDT[c]	15032.5	113.85	0.16	1	bottom	1.00	
5-field[a]	20277.8	112.04	0.66	1	bottom	1.00	σ_{yy}
5-field[b]	20277.8	113.85	0.16	1	bottom	1.82	
5-field[c]	15047.6	113.85	0.16	1	bottom	1.00	
8-field[a]	20269.1	112.04	0.66	1	bottom	1.00	σ_{yy}
8-field[b]	20269.1	113.85	0.16	1	bottom	1.82	
8-field[c]	15034.5	113.85	0.16	1	bottom	1.00	
11-field[a]	19533.4	112.04	0.66	4	top	1.00	σ_{yy}
11-filed[b]	19533.4	112.04	0.66	4	top	1.98	
11-field[c]	14539.0	112.04	0.66	4	top	1.00	
Layer	19791.7	107.52	0.56	4	top	1.00	σ_{yy}

Table 9: First-ply failure loads; all edges clamped, $[0/90]_S$ laminate under uniform transverse loading, (equilibrium stresses) $p_{xy} = 2$.

Model	FLD	Xco	Yco	Layer	Location	FI_{TW}	Max. σ
Reddy[22]	19050.9	≈5.00	≈65.00	1	top	-	
HSDT[a]	17172.8	107.51	0.56	4	top	1.00	σ_{yy}
HSDT[b]	17172.8	112.71	0.14	4	top	1.85	
HSDT[c]	12612.9	112.71	0.14	4	top	1.00	
5-field[a]	17180.3	107.51	0.56	4	top	1.00	σ_{yy}
5-field[b]	17180.3	112.71	0.14	4	top	1.85	
5-field[c]	12612.7	112.71	0.14	4	top	1.00	
8-field[a]	17175.3	107.51	0.56	4	top	1.00	σ_{yy}
8-field[b]	17175.3	112.71	0.14	4	top	1.85	
8-field[c]	12612.0	112.71	0.14	4	top	1.00	
11-field[a]	16531.3	107.51	0.56	4	top	1.00	σ_{yy}
11-filed[b]	16531.3	112.71	0.14	4	top	1.80	
11-field[c]	12322.5	112.71	0.14	4	top	1.00	
Layer	17123.6	107.51	0.56	4	top	1.00	σ_{yy}

Table 10: First-ply failure loads; all edges clamped, [-45/45/-45/45] laminate under uniform transverse loading, (direct stresses) $p_{xy} = 2$.

Model	FLD	Xco	Yco	Layer	Location	FI_{TW}	Max. σ
Reddy[22]	39354.8	≈115.	≈125.0	1	bottom	-	
HSDT[a]	39036.9	112.04	0.66	1	bottom	1.00	σ_{yy}
HSDT[b]	39036.9	119.52	0.33	1	bottom	1.65	
HSDT[c]	30258.2	119.52	0.33	1	bottom	1.00	
5-field[a]	39077.6	112.04	0.66	1	bottom	1.00	σ_{yy}
5-field[b]	39077.6	119.52	0.33	1	bottom	1.65	
5-field[c]	30281.4	119.52	0.33	1	bottom	1.00	
8-field[a]	38990.7	112.04	0.66	1	bottom	1.00	σ_{yy}
8-field[b]	38990.7	119.52	0.33	1	bottom	1.65	
8-field[c]	30224.8	119.52	0.33	1	bottom	1.00	
11-field[a]	39436.3	121.38	126.43	1	bottom	1.00	σ_{yy}
11-filed[b]	39436.3	116.81	126.85	1	bottom	1.71	
11-field[c]	30009.2	116.81	126.85	1	bottom	1.00	
Layer	39581.4	107.52	0.56	1	bottom	1.00	σ_{yy}

Table 11: First-ply failure loads; all edges clamped, [-45/45/-45/45] laminate under uniform transverse loading, (equilibrium stresses) $p_{xy} = 2$.

Model	FLD	Xco	Yco	Layer	Location	FI_{TW}	Max. σ
Reddy[22]	39354.8	≈115.0	≈125.0	1	bottom	-	
HSDT[a]	31463.7	107.51	0.56	4	top	1.00	σ_{yy}
HSDT[b]	31463.7	112.71	0.14	4	top	1.82	
HSDT[c]	23377.6	112.71	0.14	4	top	1.00	
5-field[a]	31486.1	107.51	0.56	4	top	1.00	σ_{yy}
5-field[b]	31486.1	112.71	0.14	4	top	1.82	
5-field[c]	23383.7	112.71	0.14	4	top	1.00	
8-field[a]	31403.1	107.51	0.56	4	top	1.00	σ_{yy}
8-field[b]	31403.1	112.71	0.14	4	top	1.82	
8-field[c]	23350.7	112.71	0.14	4	top	1.00	
11-field[a]	31672.2	121.38	126.43	4	top	1.00	σ_{yy}
11-filed[b]	31672.2	116.18	126.85	4	top	1.75	
11-field[c]	23955.1	116.18	126.85	4	top	1.00	
Layer	32549.2	107.51	0.56	1	bottom	1.00	σ_{yy}

Table 12: First-ply failure loads; all edges simple supported, $[0/90]_S$ laminate under uniform transverse loading, (direct stresses) $p_{xy} = 2$.

Model	FLD	Xco	Yco	Layer	Location	FI_{TW}	Max. σ
Reddy[22]	11646.5	≈5.00	≈5.00	4	top	-	
HSDT[a]	11951.7	115.65	43.66	4	top	1.00	σ_{yy}
HSDT[b]	11951.7	115.65	63.33	4	top	1.05	
HSDT[c]	11681.0	115.65	63.33	4	top	1.00	
5-field[a]	11957.0	115.46	46.18	4	top	1.00	σ_{yy}
5-field[b]	11957.0	115.65	63.33	4	top	1.05	
5-field[c]	11687.6	115.65	63.33	4	top	1.00	
8-field[a]	11952.3	115.65	43.66	4	top	1.00	σ_{yy}
8-field[b]	11952.3	115.65	63.33	4	top	1.05	
8-field[c]	11681.6	115.65	63.33	4	top	1.00	
11-field[a]	11956.6	115.65	43.66	4	top	1.00	σ_{yy}
11-filed[b]	11956.6	115.65	63.33	4	top	1.03	
11-field[c]	11755.2	115.65	63.33	4	top	1.00	
Layer	12332.8	119.20	50.27	4	top	1.00	σ_{yy}

Table 13: First-ply failure loads; all edges simple supported, $[0/90]_S$ laminate under uniform transverse loading, (equilibrium stresses) $p_{xy} = 2$.

Model	FLD	Xco	Yco	Layer	Location	FI_{TW}	Max. σ
Reddy[22]	11646.5	≈5.00	≈5.00	4	top	-	
HSDT[a]	9948.9	115.46	46.18	4	top	1.00	σ_{yy}
HSDT[b]	9948.9	117.91	62.67	4	top	1.07	
HSDT[c]	9620.2	117.91	62.67	4	top	1.00	
5-field[a]	9951.1	119.20	50.27	4	top	1.00	σ_{yy}
5-field[b]	9951.1	117.91	62.67	4	top	1.07	
5-field[c]	9623.1	117.91	62.67	4	top	1.00	
8-field[a]	9949.1	115.46	46.18	4	top	1.00	σ_{yy}
8-field[b]	9949.1	117.91	62.67	4	top	1.07	
8-field[c]	9620.5	117.91	62.67	4	top	1.00	
11-field[a]	10055.6	115.65	43.66	4	top	1.00	σ_{yy}
11-filed[b]	10055.6	117.91	62.67	4	top	1.05	
11-field[c]	9786.7	117.91	62.67	4	top	1.00	
Layer	11954.4	115.65	43.66	1	bottom	1.00	σ_{yy}

Table 14: First-ply failure loads; all edges simple supported, [-45/45/-45/45] laminate under uniform transverse loading, (direct stresses) $p_{xy} = 2$**.**

Model	FLD	Xco	Yco	Layer	Location	FI_{TW}	Max. σ
Reddy[22]	32513.5	≈115.0	≈65.0	4	top	-	
HSDT[a]	32367.0	75.09	83.33	4	top	1.00	σ_{yy}
HSDT[b]	32367.0	142.46	78.71	4	top	1.03	
HSDT[c]	31914.2	142.46	78.71	4	top	1.00	
5-field[a]	32359.6	75.09	83.33	4	top	1.00	σ_{yy}
5-field[b]	32359.6	142.46	78.71	4	top	1.03	
5-field[c]	31924.8	142.46	78.71	4	top	1.00	
8-field[a]	32463.4	71.54	50.27	4	top	1.00	σ_{yy}
8-field[b]	32463.4	142.46	78.71	4	top	1.03	
8-field[c]	32038.2	142.46	78.71	4	top	1.00	
11-field[a]	32537.5	1.20	107.16	4	top	1.00	σ_{yy}
11-filed[b]	32537.5	13.00	126.86	4	top	1.29	
11-field[c]	28595.0	13.00	126.86	4	top	1.00	
Layer	32742.6	1.20	107.16	4	top	1.00	σ_{yy}

Table 15: First-ply failure loads; all edges simple supported, [-45/45/-45/45] laminate under uniform transverse loading, (equilibrium stresses) $p_{xy} = 2$**.**

Model	FLD	Xco	Yco	Layer	Location	FI_{TW}	Max. σ
Reddy[22]	32513.5	≈115.0	≈65.0	4	top	-	
HSDT[a]	25802.4	138.28	66.13	4	top	1.00	σ_{yy}
HSDT[b]	25802.4	136.99	73.26	4	top	1.08	
HSDT[c]	24729.1	136.99	73.26	4	top	1.00	
5-field[a]	25807.7	90.62	60.86	4	top	1.00	σ_{yy}
5-field[b]	25807.7	91.91	53.73	4	top	1.09	
5-field[c]	24729.5	91.91	53.73	4	top	1.00	
8-field[a]	25687.1	90.62	60.86	4	top	1.00	σ_{yy}
8-field[b]	25687.1	91.91	53.73	4	top	1.08	
8-field[c]	24727.7	91.91	53.73	4	top	1.00	
11-field[a]	30791.5	31.22	0.56	4	bottom	1.00	σ_{yy}
11-filed[b]	30791.5	0.25	0.96	4	top	1.39	
11-field[c]	26173.7	0.25	0.96	4	top	1.00	
Layer	31078.2	1.20	107.16	4	top	1.00	σ_{yy}

The results are given in Tables 8-15. When direct stresses are used, we observe that:

1. For the initial mesh with the direct stresses computed from finite element analysis (shown with superscript a) the failure loads computed are very close to those obtained Ref. 22 for all models.
2. The locations predicted by all the models are either close to one obtained in Ref. 22 or are corresponding symmetric points.
3. The failure loads obtained by HSDT and hierarchic models are close.
4. For the same mesh the failure loads obtained by layerwise model is higher, in general, than the values obtained by HSDT and hierarchic models.
5. When the discretization error is controlled (using focussed adaptivity) for HSDT and hierarchic models, with the same initial load and adapted mesh the failure index goes above 1 (rows with superscript b). The increase in the values ranges between 1% to 98%.
6. With the adapted mesh, the failure loads reduce drastically compared to that obtained without control over discretization error (rows with superscript c). The error in the failure load can be close to 20%.
7. The failure locations for the HSDT and hierarchic models are in the same region before and after the use of discretization error control.

With equilibrium stresses we observe that:

1. For the initial mesh, the failure loads predicted by all the models are lower than those obtained in Ref. 22 (shown with superscript a) and those obtained by using direct stresses.
2. The locations predicted by all the models are either close to one obtained in Ref. 22 or are corresponding symmetric points. The locations for both direct stresses and equilibrium stresses are same (or corresponding symmetry points).
3. Failure loads predicted by the HSDT and hierarchic models are close while those predicted by layerwise are slightly higher than these.
4. When the discretization error control is used the failure index, for the failure load obtained using adapted mesh, increases upto 85%. This is due to the increased flexibility of the numerical solution for the adapted mesh.
5. With the adapted mesh the error in the failure load computations can be close to 25%.
6. The failure locations for the HSDT and hierarchic models are in the same region before and after the use of discretization error control.

It is obvious that a suitably refined mesh, along with proper post-processed values of the transverse stresses, is necessary to obtain reliable values of the first-ply failure load.

VIII. Conclusion

A comprehensive study of pointwise quality of the stress components, obtained using various families of plates models has been done. From this study it can be concluded that:

1. The pointwise displacement obtained using HSDT and hierarchic model are not very accurate for thick laminates. The accuracy improves as the plate becomes thinner. This is because of the more pronounced shear effects in thicker laminates, leading to a piecewise higher order polynomial behavior of the exact solution. The layerwise theory accurately captures this behavior for all cases.
2. The HSDT and hierarchic models are more reliable for thin plates while for thicker plates these models can lead to erroneous results.
3. The layerwise model accurately captures the local state of stress for all laminated composite plates, for different plate thickness.
4. The in-plane stress components computed by all the models are accurate, for almost all the cases.
5. The in-plane stress components computed by direct use of finite element data for layerwise model are in good agreement with exact one. The transverse stress components computed by direct use of finite element data for HSDT and hierarchic models are significantly different both qualitatively and quantitatively.
6. The equilibrium approach for computing transverse stresses is accurate for all the models.
7. Computed failure load is sensitive to the mesh, order of approximation and model used. However, proper mesh design is necessary to ensure that the local transverse stresses are computed accurately, when using post-processing.

8. When the equilibrium approach for computing transverse stresses is used the failure load computations can show reduction upto 20%.
9. When the discretization error is controlled (using focused adaptivity) failure load computed using direct stresses can go down by more than 23%.
10. When proper discretization error control is used, failure load computed using equilibrium approach for transverse stresses the failure load can go down by 25%.
11. From design point of view, proper mesh design is essential, as the actual failure load can be significantly smaller than the computed one.
12. In general, for symmetric and antisymmetric laminates, the HSDT and hierarchic models are effective, when equilibrium approach is used to obtain the transverse stresses.

References

[1]Reddy, J. N., "A simple higher order theory for laminated composite plates," *Journal of Applied Mechanics*, Vol. 51, 1984, pp. 745, 752.

[2]Szabó, B. A., and Sharmann, G. J., "Hierarchic plate and shell models based on *p*-extension," *International Journal for Numerical Methods in Engineering*, Vol. 26, 1988, pp. 1855, 1881.

[3]Ahmed, N. U., and Basu, P. K., "Higher-order finite element modeling of laminated composite plates," *International Journal of Numerical Methods in Engineering*, Vol. 37, 1994, pp 123, 129.

[4]Babuška, I., Szabó, B. A., and Actis R. L., "Hierarchic models for laminated composites," *International Journal for Numerical Methods in Engineering*, Vol. 33, 1992, pp. 505, 535.

[5]Actis R. L., Szabó, B. A., and Schwab C., "Hierarchic models for laminated plates and Shells," *Computer Methods in Applied Mechanics and Engineering*, Vol. 172, 1999, pp. 79, 107.

[6]Schwab, C., "A-Posteriori Modeling Error Estimation for Hierarchic Plate Model," *Numerische Mathematik*, Vol. 74, 1996, pp. 221. 259.

[7]Zienkiewicz, O. C., and Zhu, J. Z., "A simple error estimator and the adaptive procedure for practical engineering analysis," *Journal of Numerical Methods in Engineering*, Vol. 24, 1987, pp 337, 357.

[8]Ladevèze, P., Pelle, J. P., and Rougeot, P. H., "Error estimation and mesh optimization for classical finite elements," *Engineering Computations*, Vol. 8, 1991, pp. 69, 80.

[9]Verfürth, R., "*A review of a-posteriori error estimation and adaptive mesh refinement*," Wiley Tuebner, New York, 1996.

[10]Wahlbin, L. B., "*Local behavior in finite element methods*," In: Ciarlet, P. G., and Lions, J. L., editors. Handbook of numerical analysis, Vol. II, North Holland, 1991, pp. 357, 521.

[11]Babuška, I., Strouboulis, T., and Upadhyay, C. S., "A model study of the quality of a-posteriori error estimation for linear elliptic problem. Error estimation in the interior of patchwise uniform grids of triangles," *Computer Methods in Applied Mechanics and Engineering*, Vol. 114, 1994, pp. 307, 378.

[12]Babuška, I., Strouboulis, T., Upadhyay, C. S., and Gangaraj, S. K., "A posteriori estimation and adaptive control of the pollution error in the *h* version of finite element method," *Journal of Numerical Methods in Engineering*, Vol. 38, 1995, pp 4207, 4235.

[13]Babuška, I., Strouboulis, T., Mathur, A., and Upadhyay, C., S., "Pollution error in the *h* version of the finite element method and the local quality of a-posteriori error estimators," *Finite Element in Analysis and Design*, Vol. 17, 1994, pp. 273, 321.

[14]Mohite, P. M., and Upadhyay, C. S., "Local quality of smoothening based a-posteriori error estimators for laminated plates under transverse loading." *Computers and Structures,* Vol. 80, No.18, 19, 2002, pp. 1477, 1488.

[15]Mohite, P. M., and Upadhyay, C. S., "Focussed adaptivity for laminated plates," *Computers and Structures,* Vol. 81, 2003, pp. 287, 293.

[16]Mohite, P. M. and Upadhyay, C. S., "Accurate computation of critical local quantities in composite laminated plates under transverse loading," Communicated to *Computers and Structures*.

[17]Oden, J. T., and Cho, J. R., "Adaptive *hpq*-finite element methods of hierarchical models for plate and shell-like structures," TICAM Report 95-16, 1995.

[18]Tsai, S. W., and Wu, E. M., "A general theory of strength for anisotropic materials," *Journal of Composite Materials*, Vol. 5, 1971, pp. 55, 80.

[19]Pagano, N. J., and Hatfield, S. J., "Elastic behavior of multilayered bidirectional composites," *AIAA Journal,* Vol. 10, No. 7, 1972, pp. 931, 933.

[20]Pagano, N. J., "Exact solutions for rectangular bi-directional composites and sandwich plates," *Journal of Composite Materials*, Vol. 4, 1970, pp. 20, 35.

[21]Pagano, N. J., "Influence of shear coupling in cylindrical bending of anisotropic laminates," *Journal of Composite Materials,* Vol.4, 1970, pp. 330, 343.

[22]Reddy, Y. S. N., and Reddy, J. N., "Linear and non-linear failure analysis of composite laminates with transverse shear," *Composite Science and Technology,* Vol. 44, 1992, pp. 227, 255.